NMR Studies of Chiral P,S-Chelate Platinum, Rhodium, and Iridium Complexes and the X-ray Structure of a Palladium(II) Allyl Derivative

Alberto Albinati,† Jürgen Eckert,‡ Paul Pregosin,*,§ Heinz Rüegger,§ Renzo Salzmann,§ and Corinna Stössel§

Laboratory of Inorganic Chemistry, ETH-Zentrum, CH-8092 Zürich, Switzerland, Institute of Pharmaceutical Chemistry, University of Milan, I-20131 Italy, and Los Alamos National Laboratory, Los Alamos, New Mexico

Received September 25, 1996⊗

Several Rh(I), Ir(III), and Pt(II) complexes of the chiral P,S-bidentate ligand **2** have been prepared and characterized. Detailed two-dimensional NMR studies show that (i) the boat-type chelate ring and the stereogenic sulfur center can invert rapidly at ambient temperature and (ii) the sulfur donor may dissociate, essentially destroying the chiral pocket. The solid-state structure of [Pt(η^3-C_3H_5)(**2**)]PF_6 (**3**) has been determined and the sulfur substituent shown to have an axial orientation. The six-membered chelate ring takes up a boatlike conformation. As shown by an X-ray diffraction study for **3**, and via incoherent inelastic neutron scattering (IINS) measurements for the Pd analog, **4**, the OH group is remote from the metal atom.

Introduction

Chiral chelating ligands are now widely employed in enantioselective homogeneous catalysis.[1] Initially, diphosphine ligands predominated;[2] however, in recent studies mixed donor ligands have been shown to be advantageous.[3−7] Specifically, the development of P,O- and P,N-donor ligands has led to high observed enantiomeric excesses in allylic alkylation and Heck chemistry.[8] We have recently shown[9] that a P,S combination, in which the S-donor arises from a thioglucose, e.g. **1**, can have some utility.

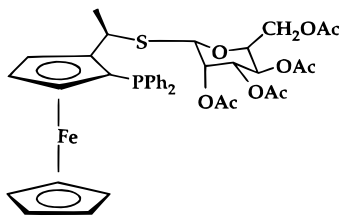

1

We have also studied ligand **2** in connection with the Pd-catalyzed allylic alkylation reaction.[1] Ligand **2** was

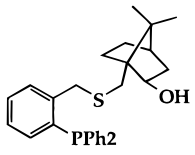

2

potentially interesting in that (i) its chirality is not associated with the phosphine backbone, (ii) it is a mixed-donor bidentate species, and (iii) there might be some interesting secondary chemistry associated with the OH function. Unfortunately, in the allylation reaction, the observed enantiomeric excesses were disappointing.[10] Since the successful design of future catalysts depends on avoiding auxiliaries prone to "err", it seemed important to trace the problems in the chemistry of this ligand. We report here on some Pt(II), Rh(I), and Ir(III) complexes of **2** and suggest that the lack of selectivity associated with **2** arises from the presence

† University of Milan.
‡ Los Alamos National Laboratory.
§ ETH Zürich.
⊗ Abstract published in *Advance ACS Abstracts,* February 1, 1997.

(1) Trost, B. M.; van Vranken, D. L. *Chem. Rev.* **1996**, *96*, 395. Togni, A.; Venanzi, L. M. *Angew. Chem.* **1994**, *33*, 497. Tanner, D. *Angew. Chem., Int. Ed. Engl.* **1994**, *106*, 625. Hayashi, T. In *Catalytic Asymmetry Synthesis*; Ojima, I., Ed.; VCH: Deerfield Beach, FL, 1993; p 325.

(2) Mackenzie, P. B.; Whelan, J.; Bosnich, B. *J. Am. Chem. Soc.* **1985**, *107*, 2046. Auburn, P. R.; Mackenzie, P. B.; Bosnich, B. *J. Am. Chem. Soc.* **1985**, *107*, 2033. Trost, B. M.; Breit, B.; Peukert, S.; Zambrano, J.; Ziller, J. W. *Angew. Chem.* **1995**, *107*, 2577. Hayashi, T.; Yamamoto, A. *Tetrahedron Lett.* **1988**, *29*, 669. Hayashi, T.; Yamamoto, A.; Ito, Y.; Nishioka, E.; Miura, H.; Yanagi, K. *J. Am. Chem. Soc.* **1989**, *111*, 6301. Togni, A.; Breutel, C.; Soares, M.; Zanetti, N.; Gerfin, T.; Gramlich, V.; Spindler, F.; Rihs, G. *Inorg. Chim. Acta* **1994**, *222*, 213. Togni, A.; Breutel, C.; Schnyder, A.; Spindler, F.; Landert, H.; Tijani, A. *J. Am. Chem. Soc.* **1994**, *116*, 4062. Togni, A.; Barbaro, P. *Organometallics* **1995**, *14*, 3570.

(3) Brown, J. M.; Hulmes, D. I.; Guiry, P. J. *Tetrahedron* **1994**, *50*, 4493. Brown, J. M.; Lloyd-Jones, G. C. *J. Am. Chem. Soc.* **1994**, *116*, 866.

(4) Rieck, H.; Helmchen, G. *Angew. Chem.* **1995**, *107*, 2881. Knühl, G.; Sennhenn, P.; Helmchen, G. *J. Chem. Soc., Chem. Commun.* **1995**, 1845. Sprinz, J.; Kiefer, M.; Helmchen, G.; Reggelein, M.; Huttner, G.; Zsolnai, I. *Tetrahedron Lett.* **1994**, *35*, 1523. Sprinz, J.; Helmchen, G. *Tetrahedron Lett.* **1993**, 1769.

(5) Lloyd-Jones, G. C.; Pfaltz, A. *Angew. Chem.* **1996**, *107*, 534. Pfaltz, A. *Acc. Chem. Res.* **1993**, *26*, 339. von Matt, P.; Pfaltz, A. *Angew. Chem., Int. Ed. Engl.* **1993**, *32*, 566. Leutenegger, U.; Umbricht, C.; Fahrni, P.; von Matt, P.; Pfaltz, A. *Tetrahedron* **1992**, *48*, 2143. Mueller, D.; Umbricht, B.; Weber, A.; Pfaltz, A. *Helv. Chim. Acta* **1991**, *74*, 232.

(6) Frost, C. G.; Williams, M. J. *Synlett* **1994**, 551. Dawson, G.; Frost, C. G.; Williams, J. M. J. *Tetrahedron Lett.* **1993**, *34*, 3149.

(7) Togni, A.; Burckhardt, U.; Gramlich, V.; Pregosin, P.; Salzmann, R. *J. Am. Chem. Soc.* **1996**, *118*, 1031. Burckhardt, U.; Hintermann, L.; Schnyder, A.; Togni, A. *Organometallics* **1995**, *14*, 5415. Abbenhuis, H. C. L.; Burckhardt, U.; Gramlich, V.; Togni, A.; Albinati, A.; Mueller, B. *Organometallics* **1994**, *13*, 4481.

(8) Loiseleur, O.; Meier, P.; Pfaltz, A. *Angew. Chem.* **1996**, *108*, 218.

(9) Albinati, A.; Pregosin, P. S.; Wick, K. *Organometallics* **1996**, *15*, 2419.

(10) Herrmann, J.; Pregosin, P. S.; Salzmann, R.; Albinati, A. *Organometallics* **1995**, *14*, 3311.

S0276-7333(96)00823-0 CCC: $14.00

Chart 1

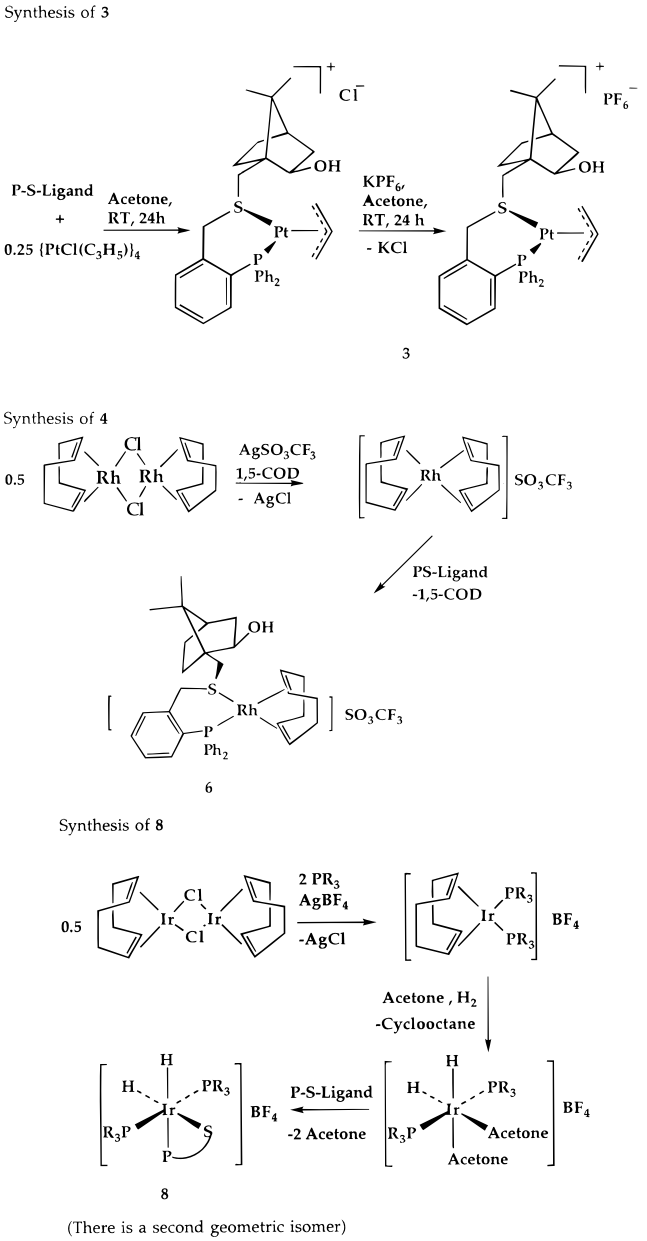

of stereoisomers due to the S atom, together with chelate ring inversion and, possibly, the propensity for this sulfur donor to dissociate.

Results

The new complexes were prepared as shown in Chart 1, using classical starting materials. Since the solution measurements were often complicated, we begin with the solid-state structure for **3**.

Solid-State Structure of [Pt(η^3-C_3H_5)(2)]PF_6 (3). The solid-state structure of **3** was determined by X-ray diffraction at 173 K, and an ORTEP view of the cation is given in Figure 1. Table 1 shows a selection of bond lengths and bond angles for **3**, whereas Table 2 gives experimental details of the structure determination. There are two different orientations of the η^3-C_3H_5 group with respect to the coordination plane, with that shown in the ORTEP having the exo structure (endo and exo refer to the orientation of the central allyl C−H bond relative to the norborneol S substituent). In the solid state the exo/endo ratio is ca. 3:1 (see Experimental Section). The immediate coordination sphere consists of the η^3-C_3H_5 allyl, the sulfur atom, and the phosphorus donor. The various bonding distances are normal: Pt−P(1), 2.264(1) Å; Pt−S, 2.318(1) Å, Pt−C(1), 2.151(6) Å; Pt−C(2), 2.169(8) Å; Pt−C(3), 2.195(5) Å. The coordination angles of interest for the major (exo) isomer are as follows: P(1)−Pt−S, 95.00(5)°; P(1)−Pt−C(1), 97.9(2)°; P(1)−Pt−C(3), 165.7(2)°; S−Pt−C(1), 167.0(2)°; S−Pt−C(3), 98.7(2)°. Within the allyl group one finds the following: C(1)−C(2), 1.36(1) Å; C(2)−C(3), 1.40(1) Å; C(1)−C(2)−C(3), 123.8(7)°. Generally, the Pt−S, Pt−P, and Pt−C(allyl) separations are in agreement with the known chelating P,S[11−13] and allyl[14−20] structural literature. Moreover, these distance and angle data for **3** are in good agreement with those for the previously reported palladium analog **4** (see Table 1). Interest-

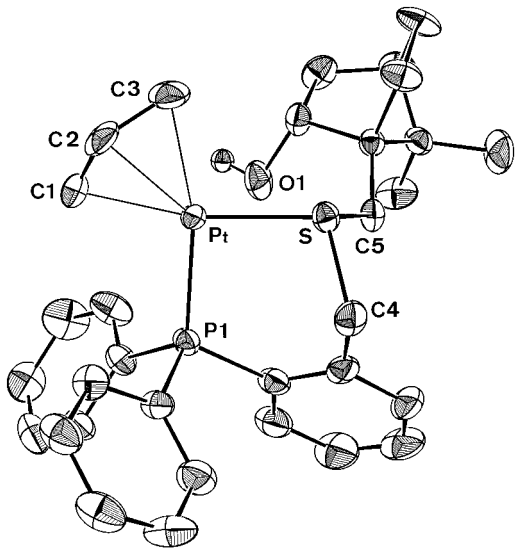

Figure 1. ORTEP view of the cation of **3**.

Table 1. Selected Bond Lengths (Å) and Bond Angles (deg) for [M(η^3-C_3H_5)(2)]$^+$

	3 (M = Pt)	**4** (M = Pd)
M−P(1)	2.264(1)	2.287(2)
M−S	2.318(1)	2.350(2)
M−C(1)	2.151(6)	2.145(9)
M−C(2)	2.169(8)	2.13(1)
M−C(3)	2.195(5)	2.198(7)
C(1)−C(2)	1.37(1)	1.34(1)
C(2)−C(3)	1.40(1)	1.41(1)
C(1)−C(2a)	1.38(2)	
C(2a)−C(3)	1.40(1)	
S−C(4)	1.839(6)	1.8559(9)
S−C(5)	1.821(5)	1.826(6)
P(1)−C(111)	1.815(5)	1.891(7)
P(1)−C(121)	1.815(5)	1.829(7)
P(1)−C(131)	1.830(6)	1.841(8)
P(1)−M−S	95.00(5)	95.41(9)
S−M−C(1)	167.0(2)	167.2(2)
S−M−C(2)	130.9(2)	132.2(2)
S−M−C(2a)	130.4(2)	
S−M−C(3)	98.7(2)	99.4(3)
P(1)−M−C(1)	97.9(2)	97.2(2)
P(1)−M−C(3)	165.7(2)	165.1(3)
C(1)−M−C(3)	68.3(2)	103.3(3)
C(1)−C(2)−C(3)	123.8(7)	124.6(9)
C(1)−C(2a)−C(3)	133(2)	
C(4)−S−C(5)	98.3(3)	
M−S−C(4)	104.5(2)	103.3(3)
M−S−C(5)	111.7(2)	112.0(2)

(11) Abel, E.; Evans, D. G.; Koe, J. R.; Sik, V.; Hursthouse, M. B.; Bates, P. A. *J. Chem. Soc., Dalton Trans.* **1989**, 2315. Abel, E.; Domer, J. C.; Ellis, D.; Orrell, K. G.; Sik, V.; Hursthouse, M. B.; Mazid, M. H. *J. Chem. Soc., Dalton Trans.* **1992**, 1073.

Table 2. Experimental Data for the X-ray Diffraction Study of [Pt(η^3-C_3H_5)(2)]PF_6 (3)

chem formula	$C_{32}H_{38}F_6OP_2PtS$
mol wt	841.7
T, K	173
space group	$P2_12_12_1$ (No. 18)
a, Å	10.815(2)
b, Å	16.121(4)
c, Å	18.736(2)
V, Å^3	3267(1)
Z	4
ρ(calcd), g cm^{-3}	1.711
μ, cm^{-1}	45.549
λ, Å	0.710 69 (graphite monochromated, Mo Kα)
θ range, deg	$2.5 < \theta < 27.0$
no. of indep data collected	3954
no. of obsd rflns (n_o)	3583 ($\|F_o\| > 5.0\sigma(\|F\|)$)
transmissn coeff	0.9998−0.9008
R^a	0.023
$R_w{}^a$	0.034

[a] $R = \sum(|F_o| - (1/k)F_c|)/\sum|F_o|$ and $R_w = [\sum w(F_o - (1/k)F_c)^2/\sum w|F_o|^2]^{1/2}$, where $w = [\sigma^2(F_o)]^{-1}$ and $\sigma(F_o) = [\sigma^2(F_o^2) + f^4(F_o^2)]^{1/2}/2F_o$.

ingly, for **4**, the Pd-P and Pd-S separations 2.287(2) and 2.350(2) Å are longer than those for **3**, the Pt analog. The distances and angles for the minor (endo) isomer do not differ significantly.

The O−H group has been localized and refined. The oxygen atom is 3.300(4) Å from the metal, and importantly, H(O1) is 3.56(6) Å from the metal and is consequently directed *away* from the platinum atom. There is no obvious hydrogen bonding between the OH group and either the PF_6^- anion or the sulfur donor; however, from the packing distances one observes somewhat short F(6)−H(O1) (2.70(7) Å) and F(4)−H(O1) (3.03(7) Å) separations. In addition, the F(3)−O(1) contact is 2.808(6) Å, which is less than the sum of the van der Waals radii for O and F.[21] We note that the O atom is sitting approximately in a pseudo fifth coordination position of the Pt atom.

The allyl plane makes an angle of 113° with the plane defined by the metal, P, and S atoms. This is normal for η^3-C_3H_5 ligands and is in agreement with the 110° value observed in **4**. The chiral P,S ligand offers an interesting chiral pocket with respect to the allyl ligand, and Figure 2 shows a space-filling model for the cation. The three allyl carbons are almost symmetrically placed with respect to the coordination plane (C(1), +0.15Å; C(2), −0.13Å; C(3), +0.15Å). The positions of the ipso carbons of the three *P*-phenyl groups (C(111), −1.67Å; C(121), +0.96Å; C(131), 0.66Å) suggest that C(111) is axial and C(121) is equatorial. The carbon bound to sulfur, C(4), is −0.72Å from the coordination plane and

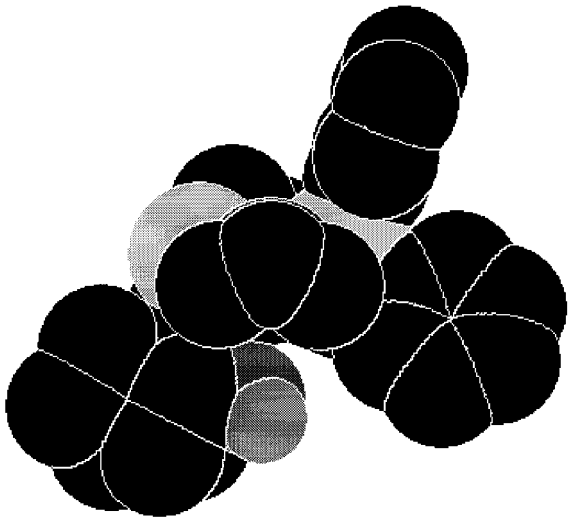

Figure 2. Space-filling model giving a view of the cation of **3**, revealing the open space around the sulfur atom (shaded).

is on the same side as C(111); C(5), at +1.67Å from the plane, completes the definition of the chiral array. The +1.67Å distance supports a pseudoaxial arrangement of this sulfur norborneol substituent.

The angles C(4)−S−C(5) (98.3(3)°), Pt−S−C(4) (104.5-(2)°), and Pt−S−C(5) (111.7(2)°) suggest that the stereochemically interesting lone pair on sulfur lies between the allyl and the exo norborneol, pointing away from the oxygen. The top area (see Figure 2) is relatively open and accommodates the sulfur lone pair. The remaining distances and angles are relatively routine.

Summarizing the structure of the chiral pocket: the two phenyl groups assume pseudoaxial and pseudoequatorial positions. The norborneol on sulfur is pseudoaxial, thus leaving a relatively large open area for the sulfur lone pair. This tendency for S-axial substituents has been noted previously.[21] The OH is directed away from the metal.

NMR Studies on [Pt(η^3-C_3H_5)(2)]PF_6 (3). The ^{31}P and ^{195}Pt NMR spectra of **3**, recorded at 323 K, show *two* components, in almost equal amounts, with ^1J(Pt,P) values of 4063 and 4059 Hz. For the discussion which follows it is useful to note the nomenclature

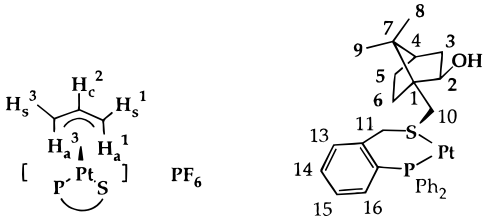

and remember that the allyl can exist in exo and endo forms.

Moreover, we will make extensive use of the dihedral angle dependence of the three vicinal coupling constants[22] shown (view down the Pt−S bond):

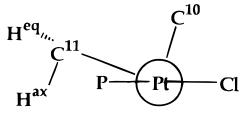

^3J(Pt,H^{11}) ^3J(P, C^{10}) ^3J(C^{10},H^{11})

(12) Chivers, T.; Edwards, M.; Meetsma, A.; van der Grampel, J.; van der Lee, A. *Inorg. Chem.* **1992**, *31*, 2156.
(13) Capdevila, M.; Clegg, W.; Gonzalez-Duarte, P.; Harris, B.; Mira, I.; Sola, J. Taylor, I. C. *J. Chem. Soc., Dalton Trans.* **1992**, 2817.
(14) Musco, A.; Pontellini, R.; Grassi, M.; Sironi, A.; Meille, S. V.; Rüegger, H.; Ammann, C.; Pregosin, P. S. *Organometallics* **1988**, *7*, 2130.
(15) Breutel, C.; Pregosin, P. S.; Salzmann, R.; Togni, A. *J. Am. Chem. Soc.* **1994**, *116*, 4067. Albinati, A.; Kunz, R. W.; Aumann, C.; Pregosin, P. S. *Organometallics* **1991**, *10*, 1800.
(16) Fernandez-Galan, R.; Manzano, B. R.; Otero, A.; Lanfranchi, M.; Pellinghelli, A. *Inorg. Chem.* **1994**, *33*, 2309.
(17) Knierzinger, A.; Schoholzer, P. *Helv. Chim. Acta* **1992**, *75*, 1211.
(18) Ozawa, F.; Son, T.; Ebina, S.; Osakada, K.; Yamamoto, A. *Organometallics* **1992**, *11*, 171.
(19) Smith, A. E. *Acta Crystallogr.* **1965**, *18*, 331.
(20) Grassi, M.; Meille, S. V.; Musco, A.; Pontellini, R.; Sironi, A. *J. Chem. Soc., Dalton Trans.* **1990**, 251; **1989**, 615.
(21) Bondi, A. *J. Phys. Chem.* **1964**, *68*, 44.

The ^{195}Pt,^{1}H interaction will help us to understand the ring conformation, whereas the ^{31}P,^{13}C and ^{13}C,^{1}H values can be diagnostic with respect to the orientation of the sulfur substituent.

The 1D-^{1}H and 2D-TOCSY NMR spectra at 323 K reveal two different η^3-allyl and norborneol moieties and somewhat broadened resonances arising from the methylene protons H_{10} and H_{11}. Surprisingly, these measurements reveal vanishingly small differences in the ^{1}H chemical shifts between analogous allyl proton resonances. This situation is incompatible with the formulation of a static chiral array as found in the X-ray structure of **3**. The heteronuclear coupling constants ^{3}J(Pt,H) for the two H_{11} protons show averaged values of ca. 75(5) Hz. If the chelate ring conformation were fixed, one would expect very different vicinal couplings, on the basis of the known dihedral angle dependence (Karplus relation) for ^{3}J(Pt,H), e.g., as indicated (view down the S−C(11) bond:

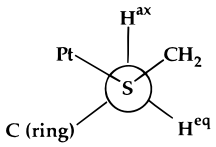

The two allyl species are in relatively *slow* exchange at 323 K, on the basis of phase-sensitive NOESY results, and we assign these two species to the exo and endo orientations of the allyl ligand.[23,24]

A series of low-temperature measurements between 183 and 293 K proved informative; unfortunately, at no single temperature was there ever a completely sharp ^{1}H spectrum. The best compromise was achieved at 233 K. At this temperature, from both the ^{31}P and ^{1}H data, there are clearly *four* isomers in solution, with similar but not quite equal populations. The various allyl ^{1}H NMR signals for **3**, together with several important protons from the ligand such as the methyl and the hydroxy groups, can be localized and assigned, using a series of 2D NMR methods (see Table 3).

At 233 K the allyl protons H_s^1 and H_a^1 are both relatively sharp and well-resolved, whereas the protons H^3 are relatively broad. Figure 3 shows the section of the 2-D proton exchange spectrum containing the syn allyl protons trans to the P-donor H_s^1 at 233 K. There are two selective exchange processes among the four isomers. Although they are not reproduced, the allyl protons H_a^1 and the norbornyl methyl signals exhibit the same type of selectivity.

At this point it seemed that the two new isomers might arise from the stereogenic sulfur atom, some preferred ring conformation, or perhaps the involvement of the OH group.

Table 3. Selected ^{1}H and ^{31}P NMR Data for [Pt(η^3-C_3H_5)(2)]$^+$ (Cation of 3)[a]

group or position	3a	3b	3c	3d
		Allyl		
1^s	4.83	4.44	4.75	4.61
1^a	2.95	3.28	3.30	2.82
2		5.22−5.28		
3^s		3.77 and 3.63		
3^a		2.88 and 2.72		
		Norborneol Fragment		
OH	2.20	2.15	2.25	2.16
2	4.04	4.11	4.11	4.05
8	0.99	0.98	0.96	1.00
9	0.74	0.77	0.71	0.78
10	2.39	2.76	2.31	2.95
10′	3.42	3.09	3.13	3.08
		Chelate		
P	14.7[b]	14.1	14.1[b]	13.4[b]
J(Pt,P)	4100	4018	4064	3992
13	7.44	7.57		

[a] In CD_2Cl_2 solution at 233 K. δ values are in ppm and J values in Hz. Isomers **3a** and **3b** are those shown in the upper half of Chart 2, whereas isomers **3c** and **3d** are in the lower half of Chart 2. [b] Assignments could be reversed.

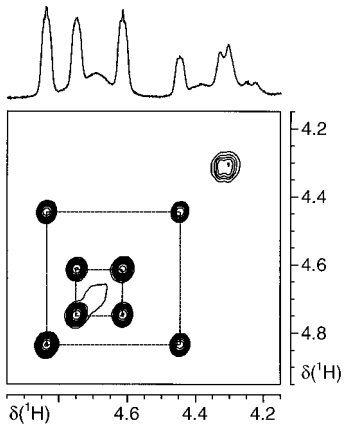

Figure 3. Section of the ^{1}H 2-D exchange spectrum showing the four allyl syn protons (each trans to phosphorus) in the four isomers of **3** (500 MHz, 233 K, CD_2Cl_2). These four protons take part in two selective exchange processes. There is an unresolved, very broad line not involved in the exchange.

Inelastic Incoherent Neutron Scattering (IINS) Studies on [Pd(η^3-C_3H_5)(2)]CF_3SO_3. Role of the OH Group. We observed earlier[10] that the Pd analog of **3**, [Pd(η^3-C_3H_5)(**2**)]CF_3SO_3 (**4**), shows selective proton NOE's from the OH group such that one might think that the hydroxy group was rigidly in place above the Pd atom. Some form of interaction with the metal center could not be excluded. Since the OH group was not localized[10] in the X-ray diffraction study for **4**, the point remained open.

In view of the well-known sensitivity[25] of inelastic incoherent neutron scattering (IINS) to proton motion, we have employed this technique to settle this question for **4**. In order to isolate the vibrational modes involving the hydroxy moiety, a sample difference technique was used (see Experimental Section). The resulting difference spectrum shows the vibrational modes of the "O−H" fragment, as well as some other modes arising from large-amplitude displacements of this group, e.g. certain ring deformations.

(22) See: Erickson, L. E.; Sarneski, J. E.; Reilley, C. N. *Inorg. Chem.* **1975**, *14*, 3007. Erickson, L. E.; Sarneski, J. E.; Reilley, C. N. *Inorg. Chem.* **1978**, *17*, 1701. Yano, S.; Tukada, T.; Yoshikawa, S. *Inorg. Chem.* **1978**, *17*, 2520 and references therein (for Karplus type relationships involving ^{195}Pt with ^{13}C and ^{1}H). For the Karplus relation and ^{3}J(^{31}P,X), see also: *Methods in Stereochemical Analysis*; Verkade, J. G., Quin, L. D., Eds.; VCH: Deerfield Beach, FL, 1987; Vol. 8.

(23) Faller, J. W. In *Determination of Organic Structures by Physical Methods;* Nachod, F. C., Zuckerman, J. J., Eds.; Academic Press: New York, 1973; Vol. 5, p 75. Vrieze, K. In *Dynamic Nuclear Magnetic Resonance Spectroscopy;* Jackman, L. M., Cotton, F. A., Eds.; Academic Press: New York, 1975.

(24) Faller, J.; Thomsen, M. E. *J. Am. Chem. Soc.* **1969**, *91*, 6871. Faller, J.; Incorvia, M. J.; Thomsen, M. E. *J. Am. Chem. Soc.* **1969**, *91*, 518.

(25) Bacon, G. E. *Neutron Scattering in Chemistry*; Butterworths: London, England, 1977.

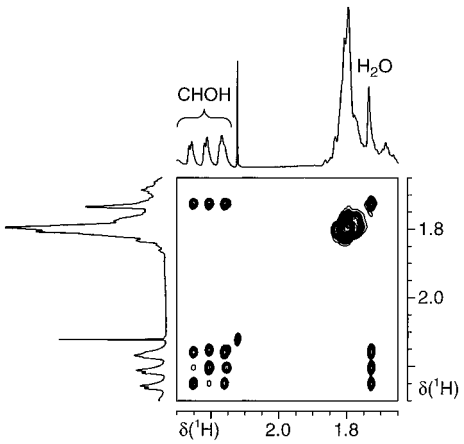

Figure 4. Section of the ^{1}H 2-D exchange spectrum for **3** showing the OH region of the spectrum. The OH resonances at high frequency are in selective exchange with each other and in nonselective exchange with traces of water (low frequency) in the solvent. The splitting on the OH signals stems from C*H*OH (500 MHz, 233 K, CD_2Cl_2).

The IINS difference spectrum has a prominent peak at 645 cm^{-1} and several overlapping bands between 700 and 1100 cm^{-1}, as well as a broad band at ca. 1560 cm^{-1}. Since the IINS band intensities are largely determined by the displacement amplitudes of the H atoms, and as these are larger for deformation modes, the peak at 645 cm^{-1} may readily be identified as the out-of-plane bending mode γ(OH) of an essentially noninteracting, non-hydrogen-bonded OH group, on the basis of its intensity.[26] The in-plane bending δ(OH), found as a broad band near 1560 cm^{-1}, is generally not affected significantly by weak interactions. Other vibrational modes involving hydroxyl displacements are found at 810, 965, and 1130 cm^{-1} and may be described as C−C−O stretches.[27]

Consequently, we conclude from the low-frequency γ-(OH) data in this complex that the OH group is not interacting with the metal through hydrogen bonding. Given this result, we reconsidered the solution exchange data for the platinum complex **3**.

Figure 4 shows the section of the solution exchange spectrum for the four nonequivalent OH protons for the isomers of **3**, at 233 K. Each of these protons is coupled to the adjacent methine CH proton. Two of these OH signals, at lower frequency, overlap somewhat; nevertheless, it is readily seen that all four are in slow exchange within themselves as well as with the small amount of free H_2O present. Consequently, the OH group plays no special role in this platinum compound, in agreement with the IINS study for the Pd analog. We assume that the relatively slow exchange of the OH group (also observable at ambient temperature) is due to a weak interaction with the anion.

$PtCl_2$(2) (5). This relatively simple complex of **2** was chosen to study the chelate ring conformation. Complex **5** exists in solution as two stereoisomers which equilibrate slowly at ambient temperature. The ^{1}H and ^{13}C resonances can be fully assigned for the major isomer (93%), and in part for the minor isomer (7%), on the basis of a combination of ^{195}Pt^{1}H, ^{31}P^{1}H, ^{13}C^{1}H, and ^{13}C^{1}H long-range correlations, together with NOESY two-dimensional experiments. NMR data for these are summarized in Table 5. The solution structure of the major isomer **5a** can be established on the basis of (i) H−H distance constraints, as evidenced by two-dimensional NOE spectroscopy, and (ii) the dihedral angle dependence of the vicinal and long-range ^{13}C^{1}H, ^{31}P^{1}H, and ^{195}Pt^{1}H coupling constants.

Specifically, the conformation of the P,S chelate six-membered ring is determined by a strong NOE between the aryl proton H_{13} and the chelate ring proton H_{11}^{eq}, plus a weak interaction between the phosphine phenyl *ortho* protons resonating at δ 7.77 and H_{11}^{ax} (see Figure 5a). The relative volumes of the appropriate NOESY cross-peaks are consistent with the distances observed in the crystal structure of **3**, i.e., 2.25 and 3.00 Å, respectively, suggesting that a static boat-type ring conformation similar to that in **3** is preserved in solution for **5a**. The values $^3J(^{195}Pt,^1H)$ for the nonequivalent ring methylene signals strongly support this assignment, as H_{11}^{eq} shows a large coupling of 116 Hz, whereas the geminal H_{11}^{ax} shows a moderate coupling of 43 Hz. These values are in agreement with the expected Karplus-like behavior for ^3J(Pt,H), noted above, and the proposed boat-type chelate ring conformation. Moreover, the ^4J(P,H) long-range coupling constant for H_{11}^{eq} (4.3 Hz) is similar in magnitude to that for H_{13} (4.6 Hz), indicative of the quasi-planar arrangement for both of these spins. We show below a fragment of the major isomer of **5**, with key protons indicated:

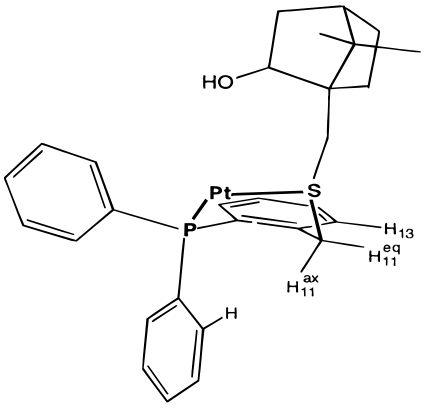

The sulfur norborneol substituent is axial, as is evident from NOE spectroscopy; e.g., H_{11}^{ax} is always distant from the norborneol moiety (see Figure 5b). This configuration at sulfur is further supported by the *absence* of a $^3J(^{31}P,^{13}C)$ coupling for C_{10} and the presence of a cross-peak in the CH long-range correlation, indicating a substantial ^3J value between C_{10} and H_{11}^{ax}. With respect to the former, it should be noted that the corresponding dihedral angle, C_{10}−S−Pt−P, from the X-ray study of **3** is 81.3°, which is close to the expected minimum in the Karplus relation, thereby suggesting the following fragment for **5a** (view down the Pt−S bond):

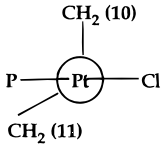

(26) Noval, A. *Struct. Bonding* **1974**, *17*, 177.
(27) Daimay Lin-Vien. *The Handbook of infrared and Raman characteristic frequencies of organic molecules*; Academic Press: Boston, 1991.

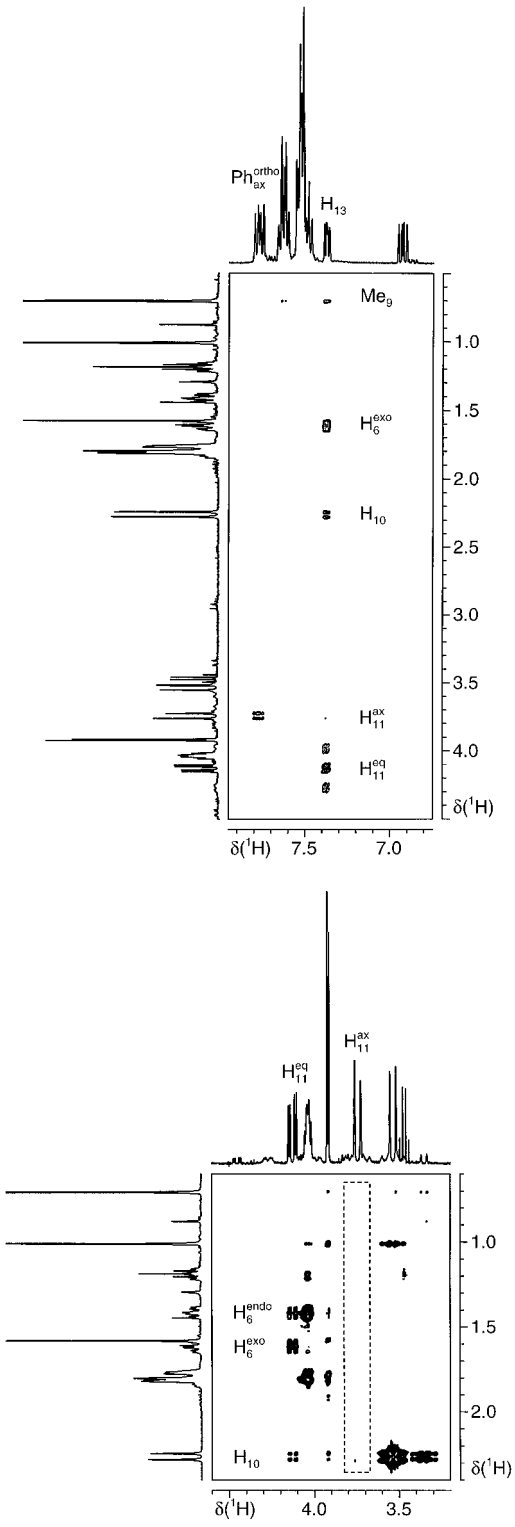

Figure 5. Sections of the NOESY spectrum of **5** showing (a, top) the selective cross-peak between $H_{11}{}^{ax}$, at ca. 3.74 ppm, and the *ortho* protons of the *P*-phenyl$_{ax}$, group, at ca. 7.7 ppm (lower left), plus the selective cross-peak due to the H_{13}/H_{11} NOE (center-bottom), thereby helping to determine the ring conformation, and (b, bottom) the absence of NOE between $H_{11}{}^{ax}$ and the norbornyl protons (dotted box), thus showing the axial nature of the S-substituent (400 MHz).

These results are all consistent with the structural fragment shown previously.

Due to its small abundance, it is not possible to deduce the structure of the minor isomer **5b** with the same rigor. However, invaluable information is obtained from (i) the HMQC $^{195}Pt^{1}H$ correlation and (ii) a $^{1}H^{1}H$ exchange experiment. The former reveals that the $^{3}J(^{195}Pt^{1}H)$ coupling constants are similar in **5a** and **5b** (see Table 4), whereas the latter shows there is relatively slow ring inversion on the NMR time scale. Figure 6 shows the ^{195}Pt satellites for H_{10} and H_{11} and, in addition, indicates that the exchange is crosswise, i.e., the equatorial proton $H_{11}{}^{eq}$ in **5a** (large $^{3}J(Pt,H)$) moves into an axial position in **5b** (small $^{3}J(Pt,H)$), and that the axial spin $H_{11}{}^{ax}$ in **5a** exchanges with proton $H_{11}{}^{eq}$ in **5b**. Figure 7 shows the appropriate exchange spectrum. Consequently, isomer **5b** has its P,S chelate ring inverted. Although not proven conclusively, it is likely that the configuration at the stereogenic sulfur center inverts *simultaneously*. In **5b**, the value $^{3}J(^{31}P,^{13}C)$ to C_{10}, the exo methylene carbon, is not resolved. This is in keeping with an axial position for C_{10}. In an equatorial position the dihedral angle would be close to 150°, thereby affording a relatively large $^{3}J(^{31}P,^{13}C)$.

The overall shape of the minor isomer has very much the same form as the major isomer. In fact, the structure for **5b** could be thought of as resulting from a reflection of the structure of **5a** and "changing" the hydroxy group from position 2 to 6. As a consequence, the "chiral pockets" of the two isomers are almost, but not quite, enantiomorphic. The source of the difference in ring-inversion energies between the allyl and dichloro complexes is not clear; however, for the latter, models suggest that the hydroxy proton could hydrogen-bond to a proximate Cl^{-}, thus adding some additional rigidity to **5**.

Table 4. ^{1}H and ^{13}C NMR Data for the Complex $[PtCl_2(2)]$[a]

	major isomer[b]					minor isomer[c]			
group or position	δ-(^{1}H)	*J*-(Pt,H)	*J*-(P,H)	δ-(^{13}C)	*J*-(P,C)	δ-(^{1}H)	*J*-(Pt,H)	*J*-(P,H)	δ-(^{13}C)
OH	3.92					1.78			
1				54.0[d]					52.6
2	4.04			75.7		4.08			76.6
3	1.81			39.6					
	1.81								
4	1.76			45.2					46.4
5	1.81			27.4					27.2
	1.19					1.12			
6	1.42			29.9		1.49			
	1.61					1.95			
7				48.8[d]					49.0
8	1.01			19.9		1.0			20.4
9	0.71			20.5		0.88			20.8
10	3.53	38		36.4		2.94	∼7		
	2.26	∼2				3.35	41		
11	4.13	116	4.3	36.4	10.5	3.82	50		
	3.74	43				4.45	107	3.9	
12				137.2	10.3				
13	7.37		4.6	133.8	8.2	7.51			
14	7.63		-	132.2[e]	3.0				
15	7.52		-	130.5	9.4				
16	6.93		11.6	135.2	5.9	6.87		11.4	
17				123.8	60.5				
$Ph_{ax}{}^{i}$				126.7	72.9				
$Ph_{ax}{}^{o}$	7.77		12.8	135.2	11.4	7.55			
$Ph_{a}{}^{m}$	7.54			129.7[f]	11.9				
$Ph_{ax}{}^{p}$	7.65			132.9	2.9				
$Ph_{eq}{}^{i}$				124.8	64.0				
$Ph_{eq}{}^{o}$	7.49			134.8	11.0	7.71			
$Ph_{eq}{}^{m}$	7.54			128.8[f]	12.3				
$Ph_{eq}{}^{p}$	7.63			132.3[e]	2.8				

[a] In $CDCl_3$ at 295 K. δ values are in ppm and *J* values in Hz. [b] $\delta(^{31}P)$ 2.3, $J(Pt,P) = 3712$, $\delta(^{195}Pt)$ −4166. [c] $\delta(^{31}P)$ 2.9, $J(Pt,P) = 3672$, $\delta(^{195}Pt)$ −4136. [d–f] Assignments could be reversed.

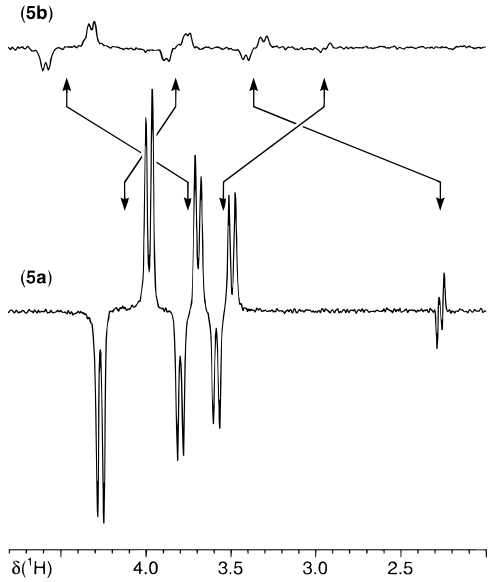

Figure 6. ^{195}Pt satellites from the HMQC spectra for **5a** (lower trace) and **5b** (upper trace). The arrows indicate which signals exchange with one another. It is obvious that there are both relatively large and relatively small $^3J(^{195}\text{Pt},^1\text{H})$ values; e.g., in the lower trace, see the first two anti-phase doublets relative to the second two anti-phase doublets. Note that the high-frequency proton in **5a** with the relatively large ^3J coupling is exchanging with a proton in **5b** with a much smaller ^3J coupling.

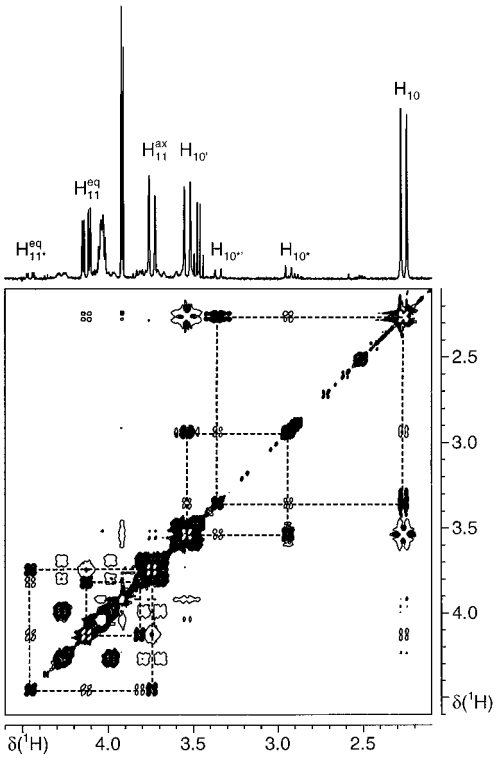

Figure 7. Section of the NOESY spectrum of **5** showing the exchange between the various H_{10} and H_{11} protons (indicated by the dotted boxes).

Given these data, it is now possible to propose structures for the four allyl derivatives **3** (Chart 2), as well as for the two isomers of **5** (Chart 3).

NMR Studies on [Rh(1,5-COD)(2)]CF_3SO_3 (6). The ambient-temperature ^{31}P NMR spectrum for the 1,5-COD complex **6** showed one sharp doublet due to

Chart 2

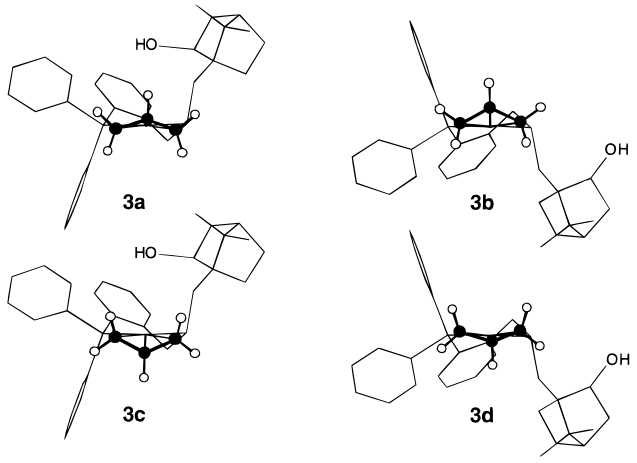

Chart 3

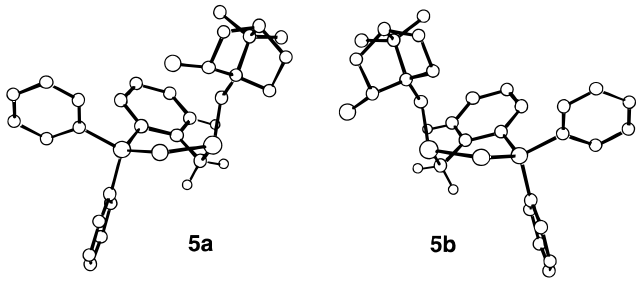

^{103}Rh coupling. The ^{1}H and the ^{13}C NMR spectra

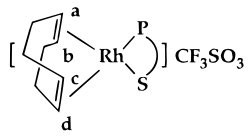

6

showed sharp resonances for both the diolefin and the coordinated ligand **2**, and these could be assigned on the basis of homo- and heteronuclear correlation experiments. Details of these NMR assignments are given in Table 5.

These results are consistent with either the presence of one single stereoisomer or, alternatively, with two isomeric forms in fast exchange on the NMR time scale. That the latter is indeed the case is evident from the following observations.

(i) The diastereotopic protons H_{11} are isochronous in $CDCl_3$ solutions, and the pairs of olefinic protons on the same double bond have almost the same chemical shifts. This points to a situation where dynamic averaging leads to the presence of a pseudo plane of symmetry coinciding with the coordination plane.

(ii) In CD_2Cl_2 solution, where the ring H_{11} protons possess slightly different chemical shifts, ^{31}P^{1}H and ^{103}Rh^{1}H correlation experiments (see Figure 8) reveal that both protons are almost equally coupled to P and Rh. A detailed analysis, shown in Figure 9, affords ^4J(P,H) values of 3.3 and 2.6 Hz and ^3J(Rh,H) values of 2.3 and 1.9 Hz for the H_{11} protons resonating at δ 3.65 and 3.58, respectively. This is clearly in contradiction to the situation encountered for **5** but reminiscent of the observations for **3**. On the basis of the spread of

Table 5. Selected NMR Data[a] for 6

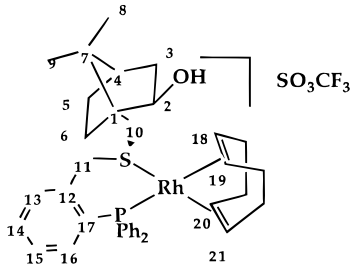

position	^{1}H	^{13}C
OH	3.77	
2	4.06	75.1
3	1.83	41.4
3′	1.83	41.4
4	1.72	45.5
5	1.75	27.1
5′	1.13	27.1
6	1.57	31.7
6′	1.40	31.7
8	1.05	20.3
9	0.78	20.3
10	2.39	36.0
10′	3.09	36.0
11	3.58	35.2, J(P,C) = 13
11′	3.58	
18	5.63	103.8
19	5.63	105.2, J(Rh,C) = 9, J(P,C) =9
20/21	3.88	87.4, J(Rh,C) = 11
21/21	3.95	88.0, J(Rh,C) = 11

[a] Endo protons are primed; $CDCl_3$ solution. Chemical shifts are in ppm and J values in Hz.

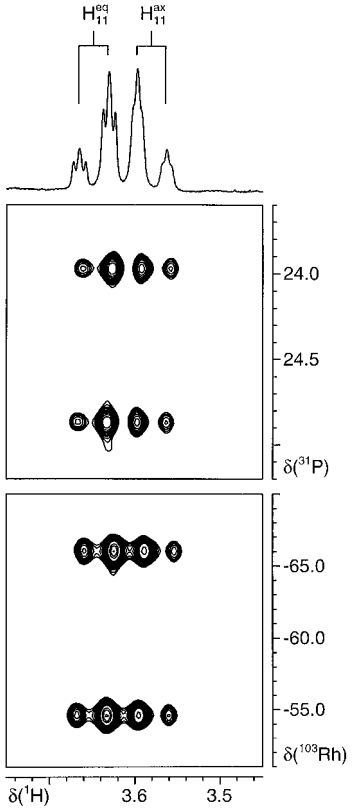

Figure 8. ^{31}P,^{1}H and ^{103}Rh,^{1}H correlations for the two H_{11} protons in **6**. The splitting in the vertical direction represents $^1J(^{103}Rh,^{31}P)$ in both cases. Note the rather similar chemical shifts for these protons.

thevicinal couplings $^3J(Pt,H_{11})$ in **3** and **5** and the assumption that the analogous $^3J(Rh,H_{11})$ values are proportionally scaled, one estimates a ratio of ca. 3:2 for the two stereoisomers **6a** and **6b**, respectively. This

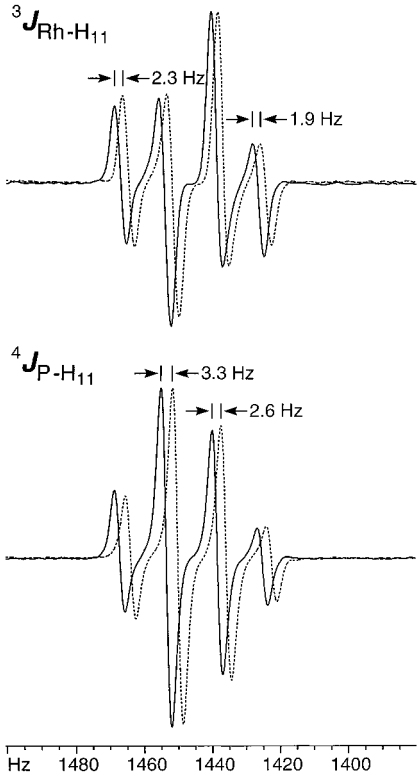

Figure 9. Detailed analysis for the two H_{11} protons in **6** (derived from Figure 8) showing the magnitudes of (a, top) the rhodium−proton spin−spin and (b, bottom) the phosphorus−proton spin−spin interactions.

ratio is in good agreement also with the averaged $^4J(P,H_{11})$ long-range coupling values.

(iii) In the NOESY spectrum (see Figure 10) one observes close contacts between the *ortho*- protons of *both* phenyl rings and the H_{11} protons, again inconsistent with a single chelate ring conformation but in agreement with the fast inversion of the boat-type chelate ring. In addition, H_{13} shows twice as many contacts as would be expected from the results for **5a**, but this is in agreement with the presence of a second isomer and fast interconversion of the two forms. It is of interest to note that the ratio of cross-peak volumes for several protons is consistently ca. 3:2.

Low-temperature NMR studies showed the presence of two separate isomers in a ratio of ca. 2:1 at 173 K. At this temperature all the ^{1}H resonances are relatively broad and exchange processes are still dominating the two-dimensional NOE spectrum. There are indications that *P*-phenyl rotation is hindered, thus complicating the interpretation.

The ambient-temperature phase-sensitive ^{1}H-NOESY spectrum for **6** reveals that the olefinic protons, shown as "a" and "b", take part in a selective slow exchange with "d" and "c", respectively.[28] However, the spins a and b do not exchange with one another. We observed similar behavior previously[29] in the chiral cationic rhodium complexes $[Rh(P,N)(diene)]^+$ (diene = 1,5-COD,

(28) Two COD protons trans to the S-donor are well resolved at 500 MHz; however, the two olefinic protons trans to the P-donor overlap. Consequently, we cannot be completely certain about the selectivity of the exchange with respect to the overlapping signals. A process in which the the two olefinic protons trans to the S-donor exchange selectively, but those trans to the P-donor exchange nonselectively, would require a rather complicated, and as yet unprecedented, mechanism.

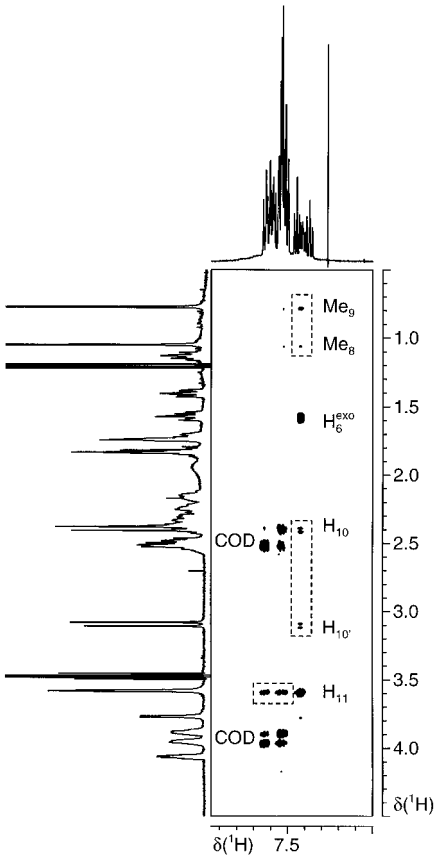

Figure 10. Section of the NOESY spectrum of **6** showing the "doubled" NOEs (dotted boxes), in the ratio ca. 3:2. The same aromatic proton is showing NOEs to very differently placed methyl groups and the two H_{10} protons (vertical boxes).

norbornadiene) with the P,N-ligand **7**. We suggested[29]

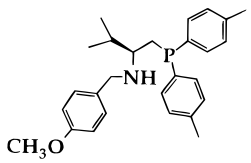

7

that the rhodium diolefin complexes of **7** isomerized via dissociation of the stereogenic secondary nitrogen atom, followed by rearrangement of the three-coordinate "T"-shaped complex and then re-formation of the four-coordinate species. We believe that an analogous mechanism is operating in **6**, i.e.

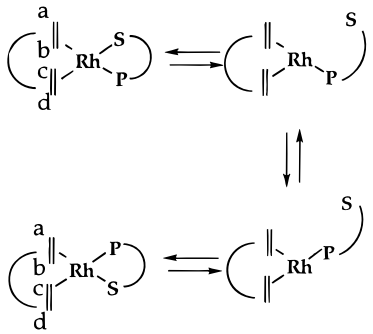

(29) Berger, H.; Nesper, R.; Pregosin, P. S.; Rüegger, H.; Wörle, M. *Helv. Chim. Acta* **1993**, *76*, 1520.

Simple ring and/or sulfur inversion, as suggested for **3** and **5a**, would change the local environments of the COD-olefinic protons, e.g. a and b, but would not rationalize the observed exchange. We cannot exclude diolefin "rotation" as a mechanism but consider this unlikely, given that several bonds must be broken simultaneously. More importantly, our results for **6** raise the question of metal−sulfur bond breaking, an additional potential contributor to poor enantioselectivity.

$[IrH_2(2)\{P(p\text{-}XC_6H_4)_3\}_2]BF_4$ (8). Relative to the chiral pocket of coordinated **2**, a square-planar coordination sphere offers a steric environment different from that found in a six-coordinate octahedral compound. Consequently, we chose to study the cations $[IrH_2(\mathbf{2})\{P(p\text{-}XC_6H_4)_3\}_2]^+$, as related dihydrides have some catalytic relevance.[30]

Reaction of the known cationic hydrogenation precursor $[IrH_2(acetone)_2\{P(p\text{-}XC_6H_4)_3\}_2]^+$ with **2** gave the octahedral complexes **8**. For X = Cl (**8a**), F (**8b**), and H (**8c**), the complexes were readily obtained in pure form; however, for X = OMe (**8d**), it was not possible to obtain an analytically pure material.

The *p*-Cl compound **8a** was analyzed in detail, although preliminary NMR results for the fluoro and hydrogen analogs suggest these are qualitatively identical. The ambient-temperature ^{31}P NMR spectrum for **8a** revealed a broad signal of relative intensity 2 at δ 5.1 and a sharp triplet of intensity 1 at δ −8.4. Empirically, we find that these two regions are typical for the ^{31}P spins of the iridium-coordinated $P(p\text{-}XC_6H_4)_3$ and **2**, respectively. At 243 K the ^{31}P spectrum shows more than 16 broad but resolvable resonances between δ +15 and −15. Many of these resonances show small splittings due to modest $^2J(P,P)_{cis}$ values.

Close inspection of the conventional ^{31}P spectrum at 243 K shows that several of the ^{31}P signals arise as a consequence of trans AB subspectra from ABX spin systems, with typical[31] $^2J(P,P)_{trans}$ values in excess of 300 Hz. Assuming, for **I**, that there are slow dynamics

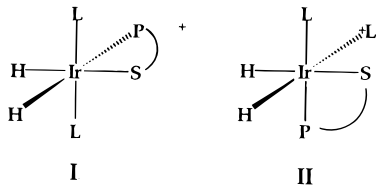

I **II**

L = P(p -XC_6H_4)3)

similar to those described above for **3** and **5**, the two monodentate arylphosphines (L) need not be equivalent; i.e., isomer **I** would readily afford two ABX ^{31}P spectra. However, these two diastereomeric isomers are insufficient to account for the more than 16 well-separated ^{31}P resonances. The data can be rationalized by assuming the presence of geometric isomer **II**, and this assumption was shown to be correct via a $^{31}P^1H$ correlation. Several of the ^{31}P resonances which revealed large $^2J(P,P)_{trans}$ values of >300 Hz correlated to protons of the P,S ligand, i.e., the ^{31}P spin of **2** was trans to an

(30) Shapley, J. R.; Schrock, R. R.; Osborn, J. A. *J. Am. Chem. Soc.* **1969**, *91*, 2816. Schrock, R. S.; Osborn, J. A. *J. Am. Chem. Soc.* **1971**, *93*, 3089.

(31) Pregosin, P. S.; Kunz, R. W. In *NMR Basic Principles and Progress*; Springer Verlag: Heidelberg, Germany, 1979; Vol. 16. Pregosin, P. S. In *Methods in Stereochemical Analysis*; Verkade, J. G., Quin, L. D., Eds.; Deerfield Beach, FL, 1987; Vol. 8.

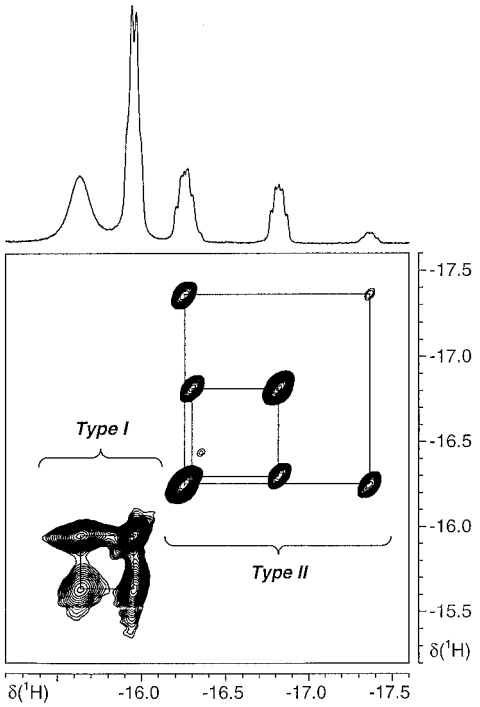

Figure 11. Section of the ^{1}H 2-D exchange spectrum for **7a** showing the hydride resonances trans to the sulfur donor. There are three selective exchange processes: one of type I and two of type II. The third (central) signal stems from two overlapping resonances (500 MHz, 243 K, CD_2Cl_2).

L ligand. In the isomers **II**, both the metal and the sulfur are stereogenic centers, thus increasing the number of possible diastereomers to four. Careful consideration of the hydride section of the ^{1}H spectra readily revealed six complexes. Together with their ^{31}P data, these hydride signals could be assigned to two type **I** and four type **II** diastereomers.

Figure 11 shows a section of the ^{1}H exchange spectrum, at 243 K, in the region of the hydride proton trans to the sulfur donor. If one accepts that the third (middle) resonance contains two overlapping signals (this is obvious from the exchange pattern), then one can see *three selective* exchange processes. Once again, we suggest that these dynamics are associated with the ring and stereogenic sulfur inversions: one pair for the major geometric isomer **I** (the two highest frequency signals in Figure 10) and two sets for geometric isomer **II** (the four lowest frequency signals). We give some NMR details for these ^{1}H hydride and ^{31}P resonances in Table 6.

We do not know the mechanism of the isomerization from **I** to **II**. Complexes **I** and **II** are not in equilibrium at 243 K (see Figure 11) but do exchange rapidly at ambient temperature, as noted above. The exchange process may involve ligand dissociation to afford a five-coordinate intermediate, followed by rearrangement and ligand recoordination. We cannot exclude isomerization via a molecular hydrogen complex. The relative abundances of **I** and **II** were found to depend on the arylphosphine with the ratios **I:II** being ca. 2:1 for X = Cl and ca. 9:1 for X = H (the latter complex measured at 253 K[32]), suggesting that the donor capability of L plays a role in determining the relative stabilities of these isomers. There are some indications, from the relative line widths in the ^{1}H and ^{31}P spectra at low temperature, that the isomers **I** may be somewhat more dynamic than those for **II**.[33] In any case, in this octahedral environment, coordinated **2** still inverts the chelate ring and, presumably, the sulfur atom quite readily.

(32) For X = OMe, the isomers **I** make up ca. 85% of the sum of **I** plus **II**; however, as noted, the sample is not pure.

Table 6. ^{1}H Hydride[a] and ^{31}P NMR Data for the Isomers I and II in the (p-ClC_6H_4)P Analog of 8 (CD_2Cl_2, 243 K)

isomer	II				I	
$\delta(H_{trans})$	−12.32	−12.13	−12.15	−12.34	−11.33	−12.02
$^2J(P,H)_{trans}$	125	121	132	125	106	125
$\delta(H_{cis})$	17.37	−16.82	−16.26	−16.31	−15.96	−15.64
$\delta(P)^b$	−10.9	−10.5		−7.6	−5.3	−5.9
$J(P,P)_{trans}$	320	308		292		
$\delta(P)^c$	3.9	4.9	8.4	−4.8	8.0	
$J(P,P)_{trans}$	315	313	296		272	
$\delta(P)^c$		12.6		5.7	10.3	
$J(P,P)_{trans}$				300	278	

[a] The descriptors cis and trans for the hydride proton are relative to the ^{31}P spin. All δ values are in ppm and J values in Hz. [b] In the chelate. [c] (p-ClC_6H_4)$_3$P.

Discussion

The Pd(II), Pt(II), Rh(I), and Ir(III) structural chemistry associated with ligand **2** involves a series of equilibrating diastereomers concerned partially with the stereogenic sulfur center. Coupled to this inversion is a simultaneous change in the chelate ring conformation. In this connection, similarities in the ^{1}H chemical shifts of the diastereotopic protons H_{11} and the lack of selectivity in the values $^3J(M,^1H)$ (M = ^{195}Pt, ^{103}Rh) have proven to be useful tools for the recognition of the rapid chelate ring flip. This interconversion can also be noted in that there is, often, an unexpected "doubling" of NOE's; i.e., a proton seems to be in contact with spatially remote sites.

Unfortunately, these equilibria can be further complicated by the presence of geometric isomers (exo/endo isomers in the Pd allyl species or cis/trans isomers in the Ir dihydride). For a given complex, it is frequently the case that the various stereo- and/or geometric isomers have similar populations; i.e., the ligands remaining in the coordination sphere do not strongly differentiate (either electronically or sterically) between the various possible isomers. There are indications, specifically from the rhodium chemistry, that this chiral P,S thioether chelate may dissociate the sulfur donor.

As **2** has a pendant hydroxy group, it was conceivable that this donor might influence the structural chemistry. However, for the Pd(II) and Pt(II) allyl complexes this seems not to be the case, as demonstrated by IINS and X-ray diffraction methods, respectively. It is possible that the hydroxy group interacts with one of the chloride ligands in **5**, thus slowing the ring inversion somewhat.

On the basis of crystallographic and MM2* results, it has been suggested[34,35] that a rigid chiral pocket is

(33) From the temperature dependence of the resonances in the hydride region, it seems clear that **I** is more dynamic than **II**; however, the complexity of the "normal" proton region does not allow us to speculate as to why this might be so.

(34) Barbaro, P.; Currao, A.; Herrmann, J.; Nesper, R.; Pregosin, P. S.; Salzmann, R. *Organometallics* **1996,** *15*, 5160.

an important quality for a successful auxiliary in connection with high enantioselectvity. For all of the various metal complexes in this study, in both square-planar and octahedral environments, 2-D ^{1}H exchange experiments reveal that coordinated **2** is sufficiently mobile, such that one cannot speak of a rigid chiral pocket. Chart 2 shows the two structures found for the dichloride complex **5**. Although the configuration at the stereogenic sulfur atom is reversed, a coordinated prochiral substrate would find little that would distinguish these two. All of our structural data, when taken together with the observed dynamics, clearly indicate that this type of chiral chelate is not likely to become (and has not yet been) a successful auxiliary.

Experimental Section

Platinum metals were obtained from Johnson-Matthey. FAB mass spectra as well as microanalytical measurements were performed in the analytical laboratories of the ETH Zurich. Solution NMR spectra were measured using Bruker AC-250 DRX 400 and AMX-500 MHz spectrometers. Referencing is to H_3PO_4 (^{31}P), TMS (^{1}H, ^{13}C), Na_2PtCl_6 (^{195}Pt) and Ξ = 3.16 MHz (^{103}Rh). Two-dimensional NMR spectra were measured, as described by us previously.[7,10,15] Mixing times in the exchange spectra were 0.5−1.0 s.

Ligand **2** was prepared as described.[10]

Crystallography. A CAD4 diffractometer was used for the unit cell and space group determination and for the data collection. A suitable crystal was mounted on a glass fiber and cooled to −100 °C by using an Enraf-Nonius FR558SH nitrogen gas-stream cryostat.

Unit cell dimensions were obtained by a least-squares fit of the 2θ values of 25 high-order reflections (9.69 ≤ θ ≤ 18.65°). Selected crystallographic and other relevant data are listed in Table 2 and Supplementary Table S1 (Supporting Information).

Data were measured with variable scan speed to ensure constant statistical precision on the collected intensities. Three standard reflections were used to check the stability of the crystal and of the experimental conditions and measured every 1 h; no significant variation was detected. Data were corrected for Lorentz and polarization factors and for decay using the data reduction programs of the MOLEN crystallographic package.[36] An empirical absorption correction was also applied (azimuthal (Ψ) scans of five reflections having χ > 88°).[37] The standard deviations on intensities were calculated in terms of statistics alone, while those on F_o were calculated as shown in Table 2.

The structure was solved by a combination of direct and Fourier methods and refined by full-matrix least squares. Moreover, from the Fourier difference maps two orientations for the allyl moiety were clearly visible. Therefore, the central carbon atom was split into two positions (C(2), C((2a)) and refined; the occupancy factors are 0.75 and 0.25, respectively. Anisotropic displacement parameters for all atoms were used during the final refinement, except for (C(2a)) which was treated isotropically.

The hydrogen atom bonded to atom O(1) was located on a Fourier difference map and refined, while for the remaining hydrogen atoms, only their contribution, in idealized positions (C−H = 0.95 Å, $B = 1.5B$(carbon) Å^2), was taken into account but not refined. The function minimized was $[\sum w(|F_o| - 1/k|F_c|)^2]$ with $w = [\sigma^2(F_o)]^{-1}$. No extinction correction was deemed necessary. The scattering factors used, corrected for the real and imaginary parts of the anomalous dispersion, were taken from the literature.[38]

The handedness of the structure was tested by refining both enantiomorphs; the coordinates giving the significantly[39] lower R_w factor were used.

Upon convergence the final Fourier difference map showed no significant peaks. All calculations were carried out by using the Enraf-Nonius MOLEN crystallographic programs.[36]

Inelastic Neutron Scattering Experiments (IINS). The IINS data were collected at the Manuel Lujan Neutron Scattering Center (MLNSC) of the Los Alamos National Laboratory.

In order to be able to distinguish the O−H vibrational modes from all the other vibrations involving hydrogen atoms of the ligands, a "*sample difference*" technique[40] was used. The method is based on the fact that the incoherent neutron scattering cross sections of hydrogen and deuterium are very different: 79.91(4) and 2.04(3) b, respectively.[41] Thus, vibrational modes involving deuterium atoms are difficult to detect by IINS in presence of many hydrogens, and the difference between two experimental IINS spectra, i.e. those of the compound containing the "O−D" and "O−H" groups, respectively, should leave only the peaks involving the modes of O−H, provided that any possible coupling of these modes to other molecular modes is negligible. However, very high counting rates are necessary, in order to obtain reasonable statistical precision on the difference data set. The filter difference spectrometer (FDS) at LANSCE[42] is particularly well-suited for this type of measurement.

In the FDS spectrometer, a pulsed "white" beam of neutrons is scattered by the sample and *energy analyzed* by a cooled Be filter, placed between the sample and the detectors. Of the scattered neutrons, only those with energies falling within the band-pass (5.2 meV, $\lambda \approx 4$ Å) of the filter analyzer will reach the detectors; the neutron final energies can thus be determined. The "time of flight" of the neutrons reaching the detectors determines the incident energies of the neutrons. The FDS spectrometer can cover an energy range from 250 to 4000 cm^{-1} with a resolution of 2−10% of the incident neutron energy.

Approximately 0.8 g of the compound [Pd(η^3-C_3H_5)(**2**)]CF_3SO_3 (**4**) and of the deuterium analogue were sealed in a cylindrical Al sample holder and maintained at ∼10 K during the data collection. Total counting times were approximately 14 h for each sample.

Pt(η^3-C_3H_5)(2)]PF_6 (3). The tetramer {PtCl(C_3H_5)}$_4$ (48.3 mg, 0.0444 mmol) and ligand **2** (81.9 mg, 0.1778 mmol) were suspended in 3 mL of acetone and stirred for 24 h at room temperature. Filtration of the resulting suspension through Celite was followed by removal of the solvent in vacuo. Addition of ether to the resulting oil produces 128 mg of a solid. This solid was collected, dissolved in 5 mL of acetone, and treated with ca. 1.2 equiv of KPF_6. After the mixture was stirred overnight, the acetone was removed and a small amount of CH_2Cl_2 added. The solids which formed (KCl, KPF_6) were filtered, and after removal of the solvent, the crude product was then recrystallized from CH_2Cl_2/ether. Yield: 97.3 mg (65.0%). Anal. Calcd (found) for $C_{32}H_{38}F_6OP_2PtS$ (MW = 841.7): C, 45.66 (45.49); H, 4.55 (4.56). IR (CsI; ν, cm^{-1}): 841 (s, P−F). MS (FAB$^+$; *m/e*): 696.5 ($M^+ - PF_6$, 100%). ^{9}F NMR (CD_2Cl_2; δ): −73.46, ^1J(P,F) = 712 Hz, PF_6^-. ^{31}P NMR (δ): 14.0, ^1J(Pt,P) = 4026 Hz.

(35) Seebach, D.; Devaquet, E.; Ernst, A.; Hayakawa, M.; Kühnle, F. N. M.; Schweizer, W. B.; Weber, B. *Helv. Chim. Acta* **1995**, *78*, 1636.
(36) MOLEN: Enraf-Nonius Structure Determination Package; Enraf-Nonius, Delft, The Netherlands, 1990.
(37) North, A. C. T.; Phillips, D. C.; Mathews, F. S. *Acta Crystallogr., Sect. A* **1968**, *24*, 351.
(38) *International Tables for X-ray Crystallography*; Kynoch: Birmingham, England, 1974; Vol. 4.
(39) Hamilton, W. C. *Acta Crystallogr.* **1965**, *17*, 502.
(40) Eckert, J. *Physica* **1986**, *136B*, 150.
(41) Sears, V. F. *Thermal Neutron Scattering Lengths and Cross-Sections for Condensed Matter Research;* Atomic Energy of Canada Ltd., Chalk River Nuclear Laboratories: Chalk River, Ontario, Canada 1984.
(42) Taylor, A. D.; Wood, E. J.; Goldstone, J. A.; Eckert, J. J. *Nucl. Instrum. Methods Phys. Res.* **1984**, *A221*, 408.

A crystal suitable for X-ray diffraction was obtained by slow diffusion of ether into a CH_2Cl_2 solution of **3**.

$PtCl_2$(2). The complex was prepared from $PtCl_2(CH_3CN)_2$ and **2** and was obtained as a colorless solid. Anal. Calcd (found) for $C_{29}H_{33}Cl_2OPPtS$ (MW = 726.6): C, 47.94 (47.66); H, 4.58(4.58). NMR data are given in Table 4.

[Rh(1,5-COD)(2)]CF_3SO_3 (6). 1,5-COD (25 μL, 0.2039 mmol) was added to a solution of $[RhCl(1,5\text{-COD})]_2$ (50.0 mg, 0.1014 mmol) and $AgSO_3CF_3$ (52.4 mg, 0.2039 mmol) in 2 mL of CH_2Cl_2 using a microsyringe. Stirring for 1 h was followed by addition of ligand **2** (94.0 mg, 0.2041 mmol) also in 2 mL of CH_2Cl_2. The previously orange suspension changed color to yellow-brown. Stirring for an additional 45 min was followed by filtration through Celite. Concentration to ca. 0.5 mL and addition of ether induces precipitation of the product as a golden powder which was dried in vacuo to afford 148 mg (89% yield of **5**. Anal. Calcd (found) for $C_{38}H_{45}O_4F_3PS_2Rh$ (MW = 838.4): C, 54.41 (54.25); H, 5.65 (5.43). MS (FAB^+ *m*/*e*): 671.9 ($M^+ - [SO_3CF_3^-]$, 30%). ^{31}P NMR (δ): 24.0, d, ^1J(Rh,P) = 145.0 Hz. IR (CsI; cm^{-1}): 3434.0 (br, OH bands); 2925 (s), 1283 (s), 1255 (s), 1156 (s), 1027 (s) 696 (m), 637 (s), 529 (m), 519 (s). ^1H and ^{13}C NMR data are given in Table 5.

General Preparation of [IrH_2(2){P(*p*-XC_6H_4)$_3$)}$_2$]BF_4 (8; X = Cl, F, H, OMe). $[IrH_2(acetone)_2\{P(p\text{-}XC_6H_4)_3\}_2]BF_4$ (0.0783 mmol) and **2** (0.0783 mmol) were dissolved in 10 mL of CH_2Cl_2 and stirred for 40 min. Concentration to ca. 1 mL was followed by addition of ether to afford a colored powder in 70−91% yield. The dihydride starting materials were obtained by passing hydrogen through cold acetone solutions (6 mL) of the bisphosphine complexes $[Ir(1,5\text{-COD})\{P(p\text{-}XC_6H_4)_3\}_2]BF_4$ for 45 min. Addition of 50 mL of ether induces precipitation of the dihydride product.

[IrH_2(2)(PPh_3)$_2$]BF_4: yield 70 mg, 70.3%. Anal. Calcd (found) for $C_{65}H_{65}BF_4IrOSP_3$ (MW = 1266): C, 61.66 (60.89); H, 5.17 (5.45). MS (FAB^+; *m*/*e*): 1179.2 ($M^+ - BF_4$, 29.9%).

[IrH_2(2)(*p*-$P(C_6H_4Cl)_3$)$_2$]BF_4: yield 105 mg, 91%. Anal. Calcd (found) for $C_{65}H_{59}BCl_6F_4IrOSP$ (MW = 1473): C, 53.00 (52.37); H, 4.04 (4.15). MS (FAB^+; *m*/*e*): 1385 ($M^+ - BF_4$, 4.8%).

[IrH_2(2)(*p*-$P(C_6H_4F)_3$)$_2$]BF_4: yield 76 mg, 71%. Anal. Calcd (found) for $C_{65}H_{59}BF_{10}IrOSP_3 \cdot H_2O$ (MW = 1392): C, 56.03 (55.10); H, 4.38 (4.29). MS (FAB^+; *m*/*e*$^+$): 1287.4 ($M^+ - BF_4$, 7.9%).

Acknowledgment. P.P. thanks the Swiss National Science Foundation and the ETH Zurich for financial support, as well as Johnson Matthey for the loan of precious metals. This work has benefited from the use of the Manuel Lujan Jr. Neutron Scattering Center, a national facility funded as such by the Department of Energy, Office of Basic Energy Sciences. A.A. acknowledges support from the CNR.

Supporting Information Available: For **3a**, a figure giving an additional view, experimental data for the X-ray diffraction study (Table S1), final positional and isotropic equivalent displacement parameters (Table S2), calculated positional parameters for the hydrogen atoms (Table S3), anisotropic displacement parameters and (Table S4), and an extended list of bond distances, bond angles, and torsion angles for **3a** (Table S5) (15 pages). Ordering information is given on any current masthead page.

OM960823Q